IOP Publishing Superconductor Science and Technology
Supercond. Sci. Technol. 32 (2019) 054004 (11pp) https://doi.org/10.1088/1361-6668/ab06a3

Effect of monotonic and cyclic axial tensile stress on the performance of superconducting CORC® wires

D C van der Laan[1,2], D M McRae[1,2] and J D Weiss[1,2]

[1] Advanced Conductor Technologies LLC, Boulder, CO 80301, United States of America
[2] Department of Physics, University of Colorado, Boulder, CO 80309, United States of America

E-mail: danko@advancedconductor.com

Received 7 November 2018, revised 22 January 2019
Accepted for publication 12 February 2019
Published 29 March 2019

Abstract

High-current superconducting CORC® wires, wound from RE-$Ba_2Cu_3O_{7-\delta}$ (REBCO) coated conductors, are being developed for use in high-field magnets that would allow operation at magnetic fields exceeding 20 T. The combination of high engineering current densities and high magnetic fields results in large Lorentz forces acting on the CORC® wire that could cause irreversible degradation to its performance. The effect of axial tensile stress on the critical current of CORC® wires containing annealed solid copper formers has been measured in liquid nitrogen to determine the irreversible stress limit at which irreversible degradation occurs. The results show no significant change in critical current before the irreversible stress limit is reached, after which the critical current decreases irreversibly with applied stress. The irreversible stress limit as high as 177 MPa depends on the yield strength of the former, the number of superconducting tapes wound into the CORC® wire and the angle at which the tapes are wound. Although the irreversible stress limit of CORC® wires is lower than a rudimentary rule of mixtures estimation would suggest, the irreversible strain limit, as high as 0.85%, exceeds that of single REBCO tapes. Both effects are likely the result of the helical fashion in which the REBCO tapes are wound into CORC® wires. The performance of CORC® wires was also measured as a function of axial tensile stress fatigue cycling in liquid nitrogen. No significant performance degradation was measured up to 100 000 cycles as long as the peak stress remained below the irreversible stress limit. Only once the peak stress was increased significantly above the irreversible stress limit would the critical current suddenly decrease with stress cycles. The results indicate that CORC® wires have matured into extremely robust high-current magnet conductors capable of withstanding high levels of axial tensile stress and strain. The irreversible stress limit of CORC® wires could be increased further by using stronger formers and winding the REBCO tapes at comparable angles, while the irreversible strain limit could potentially be increased by tailoring the winding angle of the REBCO tapes, making CORC® wires one of the strongest and most elastic high-current superconducting magnet conductors available.

Keywords: CORC® wires, axial tensile stress, fatigue cycling, high-temperature superconducting magnet cables

(Some figures may appear in colour only in the online journal)

1. Introduction

High-temperature superconductors (HTS) are required for superconducting magnets to operate at magnetic fields exceeding 20 T, or at temperatures far above the boiling point of liquid helium. Several HTS are being developed for potential use in high-field magnets, including $Bi_2Sr_2Ca_2Cu_3O_x$ (Bi-2223) tapes [1, 2], $Bi_2Sr_2CaCu_2O_x$ (Bi-2212) wires [3, 4]

and RE-$Ba_2Cu_3O_{7-\delta}$ (REBCO) coated conductors [5–7]. The main requirements for HTS materials to become feasible and practical high-field magnet conductors include high engineering current densities (J_e) of at least 300 A mm^{-2} at the operating conditions, high operating currents of between 5 and 20 kA that allow safe operation of large magnets, and high mechanical strength that prevents any degradation due to high stresses associated with operating at high currents in high magnetic fields.

Although all three HTS materials listed above allow for high operating currents and current densities, REBCO coated conductors have demonstrated by far the highest mechanical strength. REBCO coated conductors from for instance SuperPower Inc. [8] that contain a Hastelloy C-276 substrate onto which the superconducting film has been deposited have demonstrated an irreversible stress limit under axial tension (σ_{irr}) as high as 998 MPa at 77 K [9], compared to about 150 MPa for Bi-2223 tapes and Bi-2212 wires with silver alloy matrix [10, 11]. Besides critical stress, the irreversible strain limit under axial tension at which the critical current (I_c) degrades (ε_{irr}) is also an important magnet design parameter, because it determines how much strain the conductor can withstand before failure. The irreversible strain limit at 77 K of REBCO coated conductors of as high as 0.7% [9, 12] also far exceeds that of Bi-2223 tapes (about 0.3%–0.45%) [13] and Bi-2212 wires (about 0.3%) [14]. The limited mechanical strength of Bi-based conductors thus requires significant external conductor reinforcement, which reduces the overall winding current density (J_w) and therefore increases the magnet size. On the other hand, the high strength of REBCO coated conductors significantly reduces the requirements for external reinforcement, reducing the magnet design complexity and operational risk.

Large superconducting magnets, such as for use in particle accelerators, require operating currents in the order of 10–20 kA that cannot be achieved by single-tape conductors. These magnets thus require many REBCO tapes to be bundled into a high-current cable. Several approaches to cable REBCO coated conductors have been demonstrated, such as Roebel cables [15, 16], the Twisted Stacked Tape Cable [17, 18], and Conductor on Round Core (CORC®) cables and wires [19–21]. CORC® magnet cables and wires have demonstrated the ability to carry currents between 5–10 kA in background fields as high as 20 T [22, 23], while allowing for a J_e extrapolated to 20 T as high as 423 A mm^{-2} [24]. Although CORC® cables and wires contain a large number of REBCO tapes, they also contain a solid copper former that covers about 40%–60% of the conductor cross-section. While the copper fraction of around 50% may be close to the optimum value needed for stable magnet operation, it will likely lower the critical stress limit of the conductor, compared to that of single REBCO tapes.

This paper outlines the results of detailed measurements of the effect of axial tensile stress on the critical current of CORC® magnet wires in liquid nitrogen. The irreversible stress and strain limits of CORC® wires are compared to those of the REBCO tapes and the copper former from which the CORC® wires are constructed. The performance of CORC® wires under cyclic axial tensile stress loading up to 100 000 cycles is also determined in liquid nitrogen, which is an important potential failure mode for ceramic superconductors when high-field magnets are energized a large number of times throughout their lifetime. The results provide us with the current performance limits of CORC® wires and allow us to propose methods to further increase their mechanical strength.

Figure 1. Typical CORC® wire containing a solid copper former.

Table 1. CORC® wire specifications.

		CORC®-27	CORC®-30
Former size	[mm]	2.58	2.58
Tape number	[-]	27	30
Layer number	[-]	11	12
Tape width	[mm]	2	2
Substrate thickness	[μm]	30	30
Copper plating thickness	[μm]	5	5
Wire thickness	[mm]	3.7	3.8
Gap spacing	[mm]	0.3–0.4	0.3–0.4
Winding angle	[°]	30–47	30–47

2. Experimental

2.1. Preparation of CORC® wires

CORC® wires with two different layouts were prepared for this study. Both CORC® wires contained an annealed solid copper former of 2.58 mm thickness around which 27 (samples CORC®-27) or 30 (samples CORC®-30) REBCO tapes of 2 mm width were wound (figure 1) with a custom cable machine. The tapes were SCS2030 tapes from SuperPower Inc. that contained a substrate of 30 μm thickness and a surround plated copper layer of 5 μm thickness. The tapes each had a critical current of between 50 and 70 A at 77 K and were wound into 11 or 12 layers at winding angels between 30°–47° (table 1). Each tape layer was wound with opposite pitch from its neighboring layers. The CORC® wire layouts are identical to those currently developed for CORC®-based canted cosine-theta accelerator magnets [25, 26].

Figure 2. (a) CORC® wire mounted within the servo-hydraulic test fixture. (b) CORC® wire and load frame being lowered into the open liquid nitrogen cryostat.

2.2. Application of axial tensile stress

The CORC® wires were wound at lengths of several meters, after which each sample specimen was cut at a length of about 0.5 m. Copper tube terminals, 6.38 mm in diameter and 0.15 m in length, were mounted at both ends of the samples [24] and filled with 63Sn37Pb solder. Although the solder did not result in the low contact resistance typically achieved with 100In solder, its much higher mechanical strength allowed the application of the tensile stress through the terminals, without causing undue damage to the conductor within the solder under high applied loads. The terminals were clamped between two copper adapter shells that allowed homogeneous current injection. The copper adapters were mounted within the servo-hydraulic test fixture (figure 2(a)) in which the top adapter was mounted to the pull rod and the bottom adapter to the load frame of the setup. The sample and reaction frame were lowered into an open liquid nitrogen cryostat (figure 2(b)) to allow measurement of the critical current at 76 K under applied axial loads as high as 13 kN.

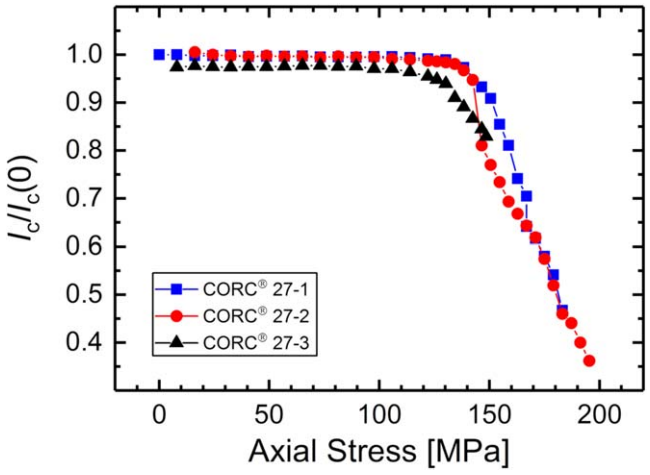

Figure 3. Critical current, normalized to its value before stress was applied, as a function of axial tensile stress of three CORC® wires containing 27 tapes, measured in liquid nitrogen.

The applied load was measured using a load cell that was mounted between the servo-hydraulic actuator and the pull rod attached to the top copper adapter mounted onto the sample. The displacement of the servo-hydraulic actuator, measured with the LVDT of the system, was used to estimate the strain of the sample. The stress applied to CORC® wires was calculated by dividing the applied force by the cross-section of the CORC® wire, assuming the CORC® wire was a solid structure without any voids. The insulation thickness of 0.025 mm was included in the calculation. The stress–strain dependence of the REBCO tapes and the copper former was measured at 76 K, in which case the sample strain was measured with a clamp-on double extensometer [27]. The measurement of the stress–strain dependence of the copper former was used as an indirect calibration of the LVDT to allow an initial estimate of the CORC® wire strain, as will be outlined in section 3.2.

3. Results

3.1. Effect of monotonic axial tensile stress on the performance of CORC® wires at 76 K

The critical current of three CORC® wires containing 27 tapes (CORC® 27-1 to CORC® 27-3) was measured as a function of axial tensile stress in liquid nitrogen. The critical current of the samples was between 1400 and 1500 A before stress was applied. No significant change in I_c was measured with increasing stress up to a stress of about 122–138 MPa (figure 3), defined as the stress at which the critical current degraded by 2%. The critical current decreased sharply once the irreversible stress limit was exceeded (table 2). No significant recovery of I_c was measured when the stress was reduced (not shown).

The dependence of I_c on axial stress of several samples containing 30 tapes (CORC® 30-1 to CORC® 30-4) measured at 76 K is shown in figure 4. The main difference between the two types of CORC® wire was the critical stress in the

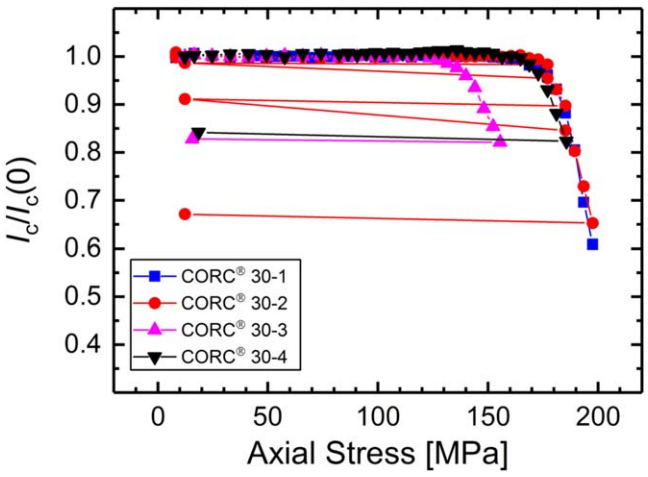

Figure 4. Critical current, normalized to its value before stress was applied, as a function of axial tensile stress of four CORC® wires containing 30 tapes, measured in liquid nitrogen.

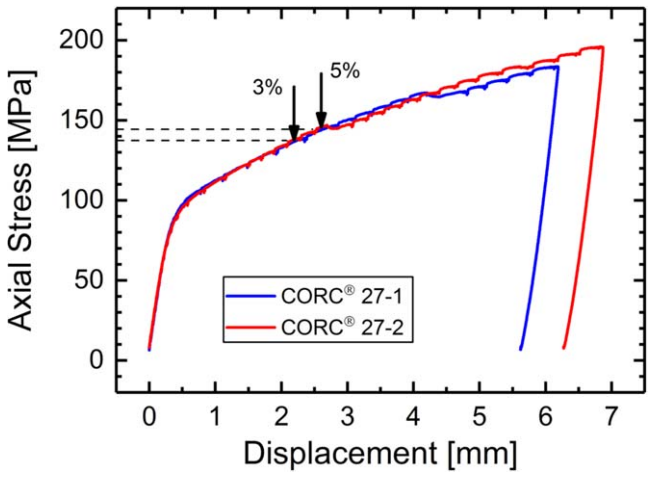

Figure 5. Axial tensile stress as a function of displacement of two CORC® wires containing 27 tapes, measured at 76 K. The arrows indicate the stress at which the critical current degraded by 3% or 5%.

Table 2. Overview of CORC® wire performance under axial stress at 76 K.

	I_c (76 K) [A]	σ_{irr} (98%) [MPa]
CORC® 27-1	1450	135
CORC® 27-2	1305	138
CORC® 27-3	1418	122
CORC® 27-4	1495	134
CORC® 30-1	1475	172
CORC® 30-2	1329	175
CORC® 30-3	1263	130
CORC® 30-4	1137	173

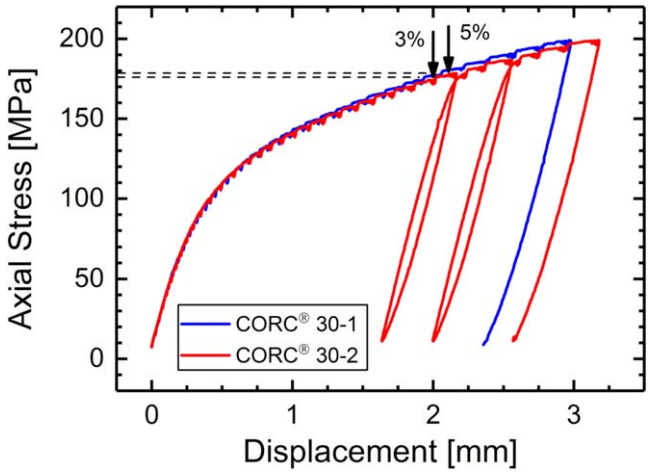

Figure 6. Axial tensile stress as a function of displacement of two CORC® wires containing 30 tapes, measured at 76 K. The arrows indicate the stress at which the critical current degraded by 3% or 5%.

30-tape CORC® wires being 26% higher than that the 27-tape CORC® wires (see table 2). Unloading the stress on sample CORC®-30 resulted in an increase in I_c of about 4 A, which is less than 0.5% of the total I_c and thus insignificant. Note that one of the 30-tape CORC® wires had a significantly lower σ_{irr} of 130 MPa, which may be caused by stress concentrations near one of the terminals.

Figure 5 shows the axial stress versus displacement, as measured with the LVDT of the servo-hydraulic actuator, of samples CORC® 27-1 and CORC® 27-2 measured at 76 K in liquid nitrogen. Although the displacement has not been converted into strain, it is clear that both samples had a yield stress of about 100 MPa, which is likely the stress at which the copper former yields. The critical current started degrading at much higher axial stress levels of between 139–145 MPa. The ripples in the stress versus displacement curves occurred when the stress was kept constant while the voltage versus current characteristic of the samples was measured to determine I_c. A similar behavior was measured in the 30-tape CORC® wires, for which the axial stress as a function of displacement of two samples is shown in figure 6.

3.2. Initial determination of the stress–strain dependence of CORC® wires at 76 K

The stress–strain dependence of the annealed copper former and of the superconducting tapes that make up the CORC® wires were measured at 76 K in liquid nitrogen. The modulus and yield stress of both components would allow us to make a first estimate of the stress–strain dependence of the CORC® wires using the rule of mixtures (ROM). Figure 7 shows the stress–strain dependence measured at 76 K of three annealed copper formers of 2.58 mm thickness. The strain was measured directly on the sample using a double clip-on extensometer. The average yield stress defined at 0.2% axial strain was 110 MPa (table 3).

Figure 8 shows the stress–strain dependence measured at 76 K of three REBCO tapes of 2 mm width containing a

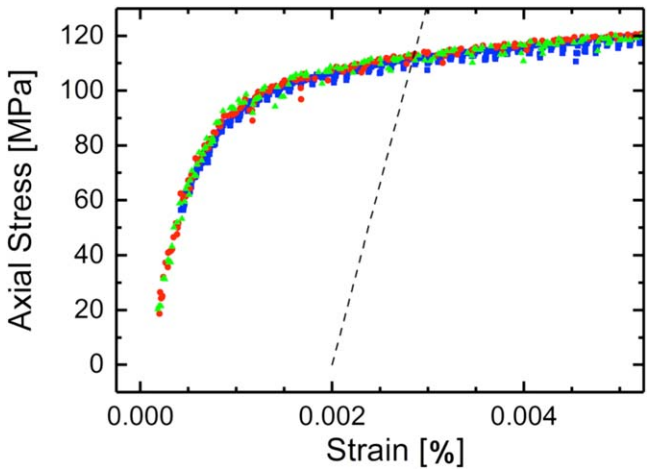

Figure 7. Stress–strain dependence measured in liquid nitrogen of the 2.58 mm thick copper former onto which the superconducting tapes were wound. The graph contains data from three samples. The dotted line allows the determination of the yield stress defined at 0.2% tensile strain.

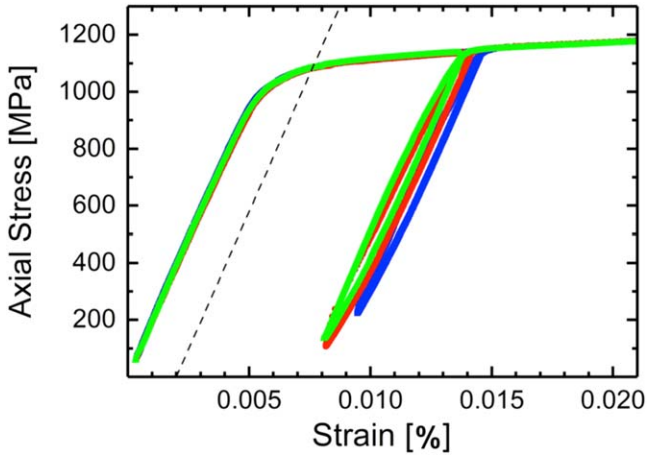

Figure 8. Stress–strain dependence measured in liquid nitrogen of the 2 mm wide REBCO tapes from which the CORC® wires were wound. The graph contains data from three samples. The dotted line allows the determination of the yield stress defined at 0.2% tensile strain.

Table 3. Yield stress of copper formers at 76 K.

		Former 1	Former 2	Former 3
Yield stress	[MPa]	110	109	110

Table 4. Yield stress of SCS2030 REBCO tapes at 76 K.

		Tape-1	Tape-2	Tape-3
Yield stress	[MPa]	1094	1093	1092

30 μm thick substrate and a 5 μm thick layer of surround plated copper. The strain was also measured directly on the sample with a pair of clamp-on extensometers. The Hastelloy

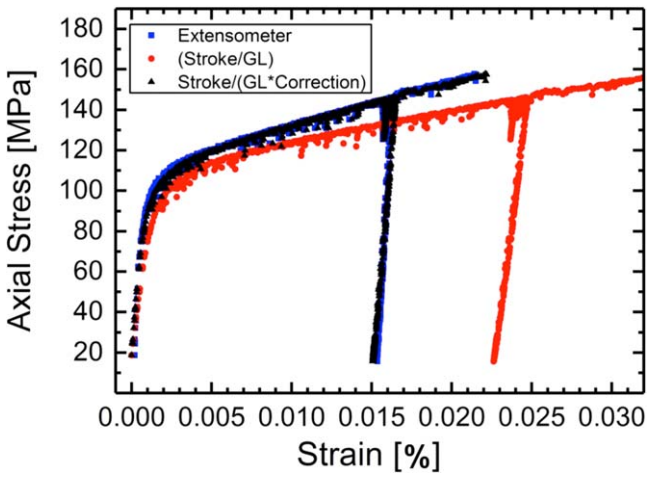

Figure 9. Stress–strain dependence of a solid copper former measured at 76 K. The strain is determined using a pair of clamp-on extensometers and the displacement of the servo-hydraulic piston divided by the grip length (GL).

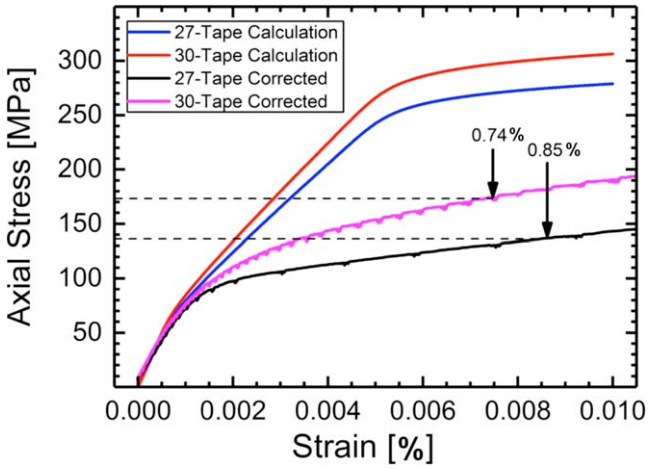

Figure 10. Stress–strain dependence of the two CORC® wires measured at 76 K after the piston displacement has been converted into strain (corrected). The graph also includes the calculated stress–strain dependences of both CORC® wires using the rule of mixtures (calculation).

C-276 substrate resulted in a relatively high yield stress of the REBCO tape of 1093 MPa (table 4).

The stress–strain measurement performed on the copper former allows an indirect calibration of the LVDT of the servo-hydraulic actuator and provides us with an estimate of the axial strain applied to the CORC® wires. Figure 9 shows the stress–strain dependence of one of the copper formers measured in liquid nitrogen. The applied strain determined using the pair of clamp-on extensometers is about 60% smaller than calculated by dividing the displacement of the servo-hydraulic piston as indicated by the LVDT by the grip length of the CORC® wire (GL). Applying a correction factor to the applied strain as determined from the piston displacement results in a very good agreement between the stress–strain curves resulting from the extensometers and LVDT. This correction factor was also applied to the measurements

performed on the two types of CORC® wires (figure 10), which results in an irreversible strain limit of sample CORC®-27 of about 0.85%, and of about 0.74% for sample CORC®-30. The irreversible strain limit of the two CORC® wires is significantly higher that measured on individual REBCO tapes at 76 K, with ε_{irr} being about 0.7% [9, 12]. The uncertainty in corrected strain is less than ± 0.05%, which is determined by a combination of the uncertainty of the strain as measured with the extensometers and the homogeneity of the sample over its length. Inhomogeneous samples could experience higher degrees of deformation outside the gage length of the extensometers, causing a large deviation between the stress–strain curve measured by the extensometer and that measured by the displacement of the piston after correction. A more detailed determination of the CORC® wire stress–strain dependence is planned for the near future.

The estimated stress–strain dependence of CORC® wires at 76 K was calculated from the mechanical properties of the former and tapes using the ROM for both sample layouts (CORC®-27 and CORC®-30), assuming that the tapes and the former are in line with the applied load. The measured stress–strain dependences of the former and individual tapes were fitted using the Ramberg–Osgood relationship:

$$\varepsilon(\sigma) = \frac{\sigma}{E} + \alpha\frac{\sigma}{E}\left(\frac{\sigma}{\sigma_0}\right)^{(n-1)}, \quad (1)$$

with ε being strain, σ stress, E Young's modulus, σ_0 yield strength, and α and n material dependent constants. The stress–strain characteristics for the tape and former were obtained by dividing the stress by the sample cross-section. The stress–strain characteristics of the 27 and 30 –tape CORC® wires were calculated by adding the load versus strain characteristics of the former and either 27 or 30 tapes, followed by division of the CORC® wire cross-section, which includes the heat shrink tube that surrounds the conductor and the gaps between tapes. The calculated and measured stress–strain dependence of both types of CORC® wires are within reasonable agreement for axial stresses of less than about 80 MPa (figure 10), which is below the yield stress of the copper former. The calculated CORC® wire stress far exceeds that of the measured CORC® wire stress for both samples once the applied stress exceeds the yield stress of the former (110 MPa). The calculated stress shows a second linear section of the stress–strain curve before the REBCO tapes yield at an applied stress of about 260–290 MPa, depending on sample layout. No such second linear part of the stress–strain curves are measured on the two types of CORC® wires. The calculated stress at high strain (1%) is about 90% higher than the measured stress for sample CORC®-27 and about 60% higher for sample CORC®-30.

The differences in calculated and measured CORC® wire stress are a direct result of the tapes in the CORC® wires being wound in a helical fashion, opposed to being parallel to the former. Under application of tensile stress to the CORC® wire, the tapes act as springs that are prevented from extending freely by the copper former located within their interior. The tapes therefore are not able to reinforce the CORC® wire to the same extent as assumed in the ROM calculation in which the straight tapes are oriented in line with the stress.

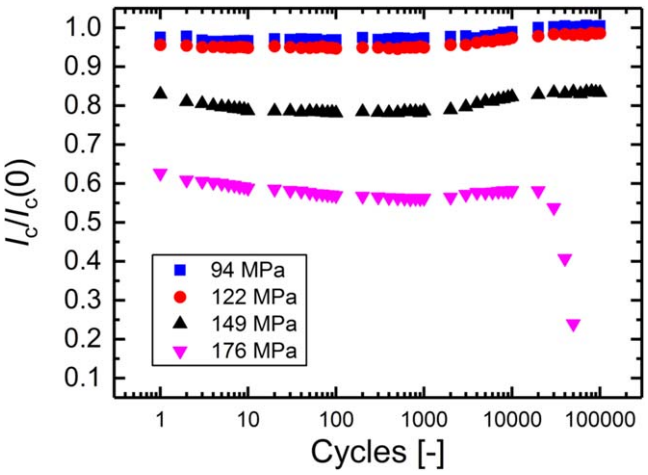

Figure 11. The effect of axial tensile stress cycling performed in liquid nitrogen on the critical current of sample CORC® 27-3 at different peak stresses. The critical current is normalized to its initial value before stress was applied.

3.3. Effect of cyclic axial tensile stress on the performance of CORC® wires at 76 K

The effect of axial tensile stress cycling on the critical current of CORC® wires was measured in liquid nitrogen at 76 K. Measurements were performed at a stress ratio of 0.1, in which case the stress was cycled between the peak stress, corresponding to a pre-determined percentage of the critical stress, and 0.1 times the peak stress. Stress cycling was performed at frequencies up to 5 Hz in liquid nitrogen up to 100 000 cycles.

Figure 11 shows the dependence of I_c as a function of cycle number for different peak stresses applied to sample CORC® 27-3. The first measurement was performed at a peak stress of 94 MPa, which corresponds to about 77% of the critical stress. No significant change in I_c, normalized to its value before stress was applied, was measured after 100 000 cycles. The critical current degraded by about 2% after the peak stress was increased to 122 MPa, which corresponds to the critical stress. Again, no significant change in I_c was measured with stress cycling. Even when the peak stress was increased to 122% of σ_{irr} (149 MPa), and I_c degraded by about 15% before cycling, I_c did not degrade further with stress cycling. Only once the peak stress was increased to 144% of σ_{irr} (176 MPa) did I_c suddenly decrease sharply after about 20 000 stress cycles. The critical current decreased from about 60%–65% to about 23% of its initial value at 50 000 stress cycles, after which the sample broke. Figure 12 shows the location of the break being close to one of the terminals.

The critical current of sample CORC® 27-3 did change during stress cycling at peak stresses of 149 and 176 MPa, but recovered before the 100 000 cycles were completed, or before I_c degraded sharply before the sample broke. The gradual reduction in I_c was as much as 10% of its initial value, but fully recovered before the 100 000 cycles were completed.

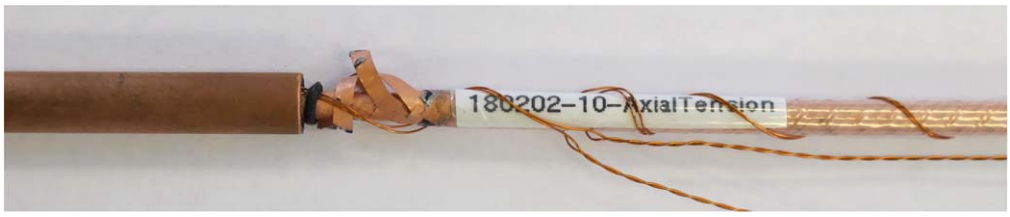

Figure 12. Location where sample CORC® 27-3 broke after 50 000 stress cycles at a peak stress of 176 MPa.

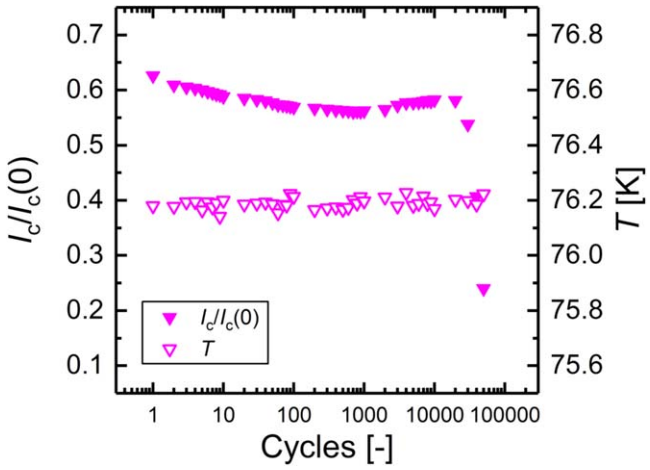

Figure 13. The effect of axial tensile stress cycling performed in liquid nitrogen on the critical current of sample CORC® 27-3 at a peak stress of 176 MPa. The critical current is normalized to its initial value before stress was applied. The graph includes the temperature of the liquid nitrogen bath at the location of the sample.

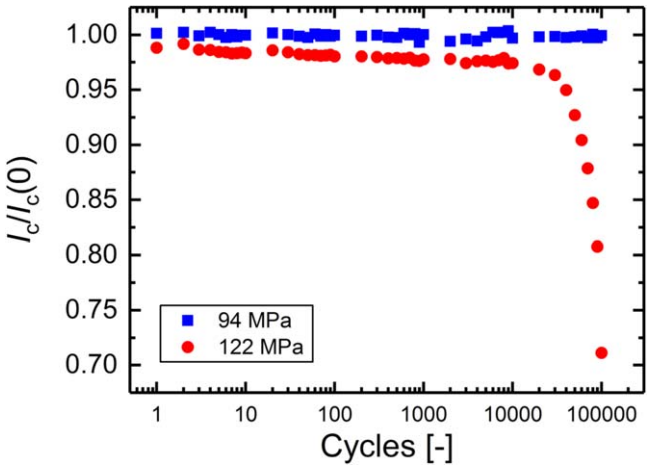

Figure 14. The effect of axial tensile stress cycling performed in liquid nitrogen on the critical current of sample CORC® 27-4 at different peak stresses. The critical current is normalized to its initial value before stress was applied.

The cause of the gradual change in I_c could potentially be caused by a change in temperature (T) of the liquid nitrogen bath with column height or atmospheric pressure. The temperature of the liquid nitrogen bath was thus measured at the location of the sample to rule out a potential change in temperature (figure 13). No correlation was found with the change in I_c and temperature, which remained constant within 0.05 K. The exact cause of the gradual decrease in I_c with stress cycling, followed by a full recovery, remains unknown. Changes in contact resistance between the tapes and the terminals with stress cycling, or in local strain state of the tapes, need to be investigated in more detail before the source can be identified.

The peak stress at which I_c of CORC® wires degrades sharply with stress cycling varied between samples, but degradation with stress cycling only occurred at peak stresses equal or greater than σ_{irr}. Figure 14 shows the dependence of I_c on stress cycling measured in liquid nitrogen of sample CORC® 27-4. A sharp degradation in I_c occurred after 20 000 stress cycles to σ_{irr} (122 MPa).

The dependence of I_c on axial tensile stress cycling was also measured on several CORC® wires containing 30 tapes (samples CORC® 30-4 and CORC® 30-5). As outlined in figures 15 and 16, the results were very similar to those measured on CORC® wires containing 27 tapes, except that they could withstand higher peak stresses. Figure 17 shows the location at which the two samples containing 30 tapes broke, one of which showing failure close to one of the terminations, while the other sample broke near the middle of the CORC® wire.

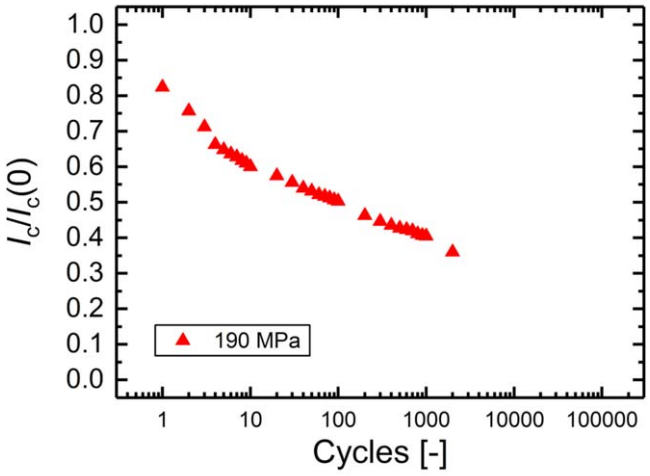

Figure 15. The effect of axial tensile stress cycling performed in liquid nitrogen on the critical current of sample CORC® 30-4 at a peak stress of 190 MPa. The critical current is normalized to its initial value before stress was applied.

The sudden collapse of the CORC® wire I_c with stress cycling at, or above σ_{irr}, is very similar to what has been reported earlier on single REBCO tapes [28–30]. On the other hand, the decrease in I_c with axial stress cycling is much more sudden, compared to the much more gradual decrease in I_c under transverse compressive stress cycling [31]. The

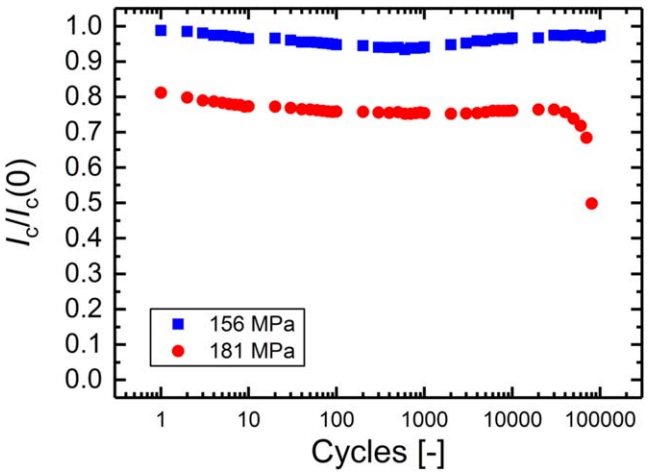

Figure 16. The effect of axial tensile stress cycling performed in liquid nitrogen on the critical current of sample CORC® 30-5 at different peak stresses. The critical current is normalized to its initial value before stress was applied.

difference can potentially be explained by the failure mode, where under axial tension cracks in the superconducting film form due to yielding of the Hastelloy substrate. On the other hand, under transverse compression the REBCO layer fails because the irreversible strain limit under axial compression is exceeded. The rate at which cracks propagate in the REBCO layer with stress cycling is apparently very different between the two failure modes.

4. Discussion

4.1. No reversible strain effect measured in CORC® wires under axial tension

The critical current of the CORC® wires remained constant under application of axial stress until the stress exceeded σ_{irr} (figures 3 and 4). I_c did not show any significant recovery after I_c degraded and the axial stress was reduced. This behavior is in contrast to the reversible strain effect of I_c measured in single REBCO coated conductors with the application of axial tensile strain [32–34], where I_c changes reversibly by as much as 10% before σ_{irr} is reached. The reason for the reversible strain effect on I_c to not occur in CORC® wires is that the winding angle of the tapes varies between 30°–47°, measured normal to the CORC® wire axis (figure 18). The reversible strain effect in most REBCO coated conductors vanishes when strain is applied at 45° with respect to the tape axis [35, 36], causing the relatively high winding strain in CORC® wires to not affect I_c. Axial stress applied to the CORC® wire also will not significantly affect I_c of the tapes, because at a tape winding angle of 45°, the stress applied along the CORC® wire axis is also oriented at an angle of 45° with respect to the tape axis. The tape winding angle in CORC® wires thus has the advantage that both the winding and the operating strains will not affect I_c until the strain exceeds the irreversible strain limit.

4.2. Performance of tapes extracted from CORC® wires

The tapes were extracted from the CORC® wires and their I_c values were measured after the CORC® wires were subjected to monotonic axial stress to determine in which layer the tape performance degraded most. Extracted tape measurements could not be performed for CORC® wires that were subjected to axial stress cycling, because failure in the CORC® wire during stress cycling was abrupt and always resulted in tape breakage at the end of the test.

Figure 19 shows the I_c values of tapes extracted from three CORC® wires that were subjected to various axial stress levels exceeding σ_{irr} that resulted in different levels of CORC® wire I_c degradation. Layer 1 corresponds to the innermost layer where tapes were wound directly onto the former, while layers 11 or 12 correspond to the outermost layer of the CORC® wires. The sum of the extracted tape I_c was comparable to the wire I_c at the end of the test (table 5), confirming that degradation did not occur near the terminals due to stress concentrations.

The majority of the tape degradation was concentrated within the tape layers at the transition where a third tape was wound into the layer, starting with layer 7. The first layer containing three tapes showed the most degradation, followed by the second layer containing three tapes (layer 8). Surprisingly, also the last layer containing two tapes (layer 6) often showed a large decrease in tape I_c. The tapes in layers 7 and 8 were wound at the highest winding angle of 47° and 45.5° respectively, while the tapes in layers 1–6 were wound at angles ranging from 30° to 35.5°. Tapes that are wound at higher angle, and are thus oriented more in the direction of the applied stress, likely experience higher stresses after the former yields compared to tapes that are wound at lower angles.

4.3. Improvement of CORC® wire irreversible stress and strain limits

The irreversible stress limit of CORC® wires containing annealed copper formers that were not optimized for high axial strength already exceeded 130–170 MPa depending on their tape count. The irreversible stress limit of CORC® wires is up to about 50% higher than that measured on a 15-strand Roebel cable [37], but only about 50% of the critical stress measured in a twisted stack of 1 mm wide tapes [38]. Stress concentration at the corners of the Roebel strands caused irreversible degradation at a much lower tensile strain (0.36%) than is measured in REBCO coated conductors, while CORC® wires could withstand higher strains of up to 0.85%.

The mechanical strength of CORC® wires could be significantly improved when using stronger metal formers, because the REBCO tapes only start to carry significant load once the former has yielded significantly. Hardened copper, or copper alloys could be considered to significantly increase the yield stress of the former and thus the critical stress of the CORC® wire. For instance, the yield stress of cold worked oxygen free copper at 76 K could be as high as 400 MPa, depending on the cold work percentage [39]. Copper alloys,

Figure 17. (a) Location where sample CORC® 30-4 broke after 2000 stress cycles at a peak stress of 190 MPa. (b) Location where sample CORC® 30-5 broke after 80 000 stress cycles at a peak stress of 181 MPa.

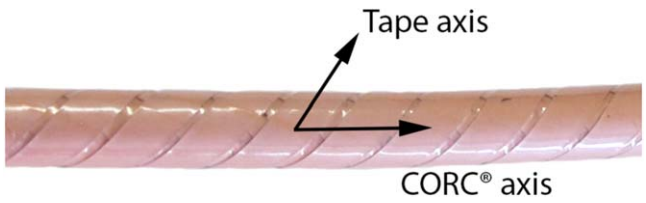

Figure 18. Orientation of the tape axis with respect to the CORC® wire axis along which stress is applied.

such as 37% cold worked CuBe C17510 would provide the former with a yield stress at 76 K of more than 700 MPa [39]. The axial stress tolerance of CORC® wires could also be increased by further optimizing the winding angles of the tapes in each layer, such that all tapes in the CORC® wire are being loaded at the same applied stress, instead of loading a small percentage of the tapes that are wound at high angle before tapes that are wound at lower angle are loaded.

The higher irreversible strain limit measured in CORC® wires compared to REBCO tapes could have multiple origins. The REBCO layer in the tapes wound into a CORC® wire is under significant axial compressive strain, as high as −1.16% for the tapes in the inner layer. Although this high compressive strain could be seen as a significant buffer against applied axial strain, the winding strain is oriented normal to the CORC® wire axis and thus normal to the applied stress. The high axial compressive strain of the REBCO layer may therefore not result in a much larger irreversible strain limit of the CORC® wire. The more likely reason why the irreversible strain limit of CORC® wires is higher than that of REBCO tapes is the helical fashion at which the tapes are wound. The tapes act as springs that extend more easily when the CORC® wire is strained, compared to straight REBCO tapes, although the extension of the spring is limited by the former that is confined within the bundle of springs. The irreversible strain limit of CORC® wires could potentially be increased even further by optimizing the winding angle of the tapes. The tapes could be wound at lower winding angles, while at the same time the variation in winding angles should be minimized. A more detailed measurement campaign, supported by modeling of the strains and stresses of each tape in the CORC® wire, should be performed to potentially extend the irreversible strain limit of CORC® wires under axial tension to even higher levels.

5. Conclusions

The effect of axial tensile stress on the critical current of CORC® wires containing an annealed solid copper former was measured in liquid nitrogen. The critical current of the CORC® wires did not change significantly until after the former yielded and the irreversible stress limit was reached, at which point the critical current degraded rapidly with axial tensile stress. Unloading the stress did not show any significant recovery of the critical current. The absence of a reversible strain effect on the critical current in CORC® wires, which is often measured in REBCO tapes, is explained by the winding angle of the tapes in CORC® wires being close to 45° with respect to the tape and thus CORC® wire axes. At this angle the reversible strain effect in REBCO tapes disappears.

The irreversible stress limit of between 130 and 170 MPa, depending on CORC® wire layout, is lower than what the ROM, based on the mechanical properties of the copper former and REBCO tapes at 76 K, would suggest. A yield stress of the annealed copper former of about 110 MPa and of about 1093 MPa for the REBCO tapes was measured at 76 K. These values would result in a calculated critical stress of the CORC® wires of between 260 and 290 MPa, depending on the CORC® wire layout. The difference between the calculated and measured irreversible stress limits can be explained by the helical fashion in which the tapes are wound into the CORC® wire, compared to being parallel to the former when using the ROM. The helical winding also likely results in a high irreversible strain limit of as high as 0.74%–0.85% in the CORC® wires compared to individual REBCO tapes.

CORC® wires were subjected to axial tensile stress cycling in liquid nitrogen. No significant reduction in CORC® wire critical current was measured even under fatigue up to 100 000 cycles as long as the peak stress remained below the

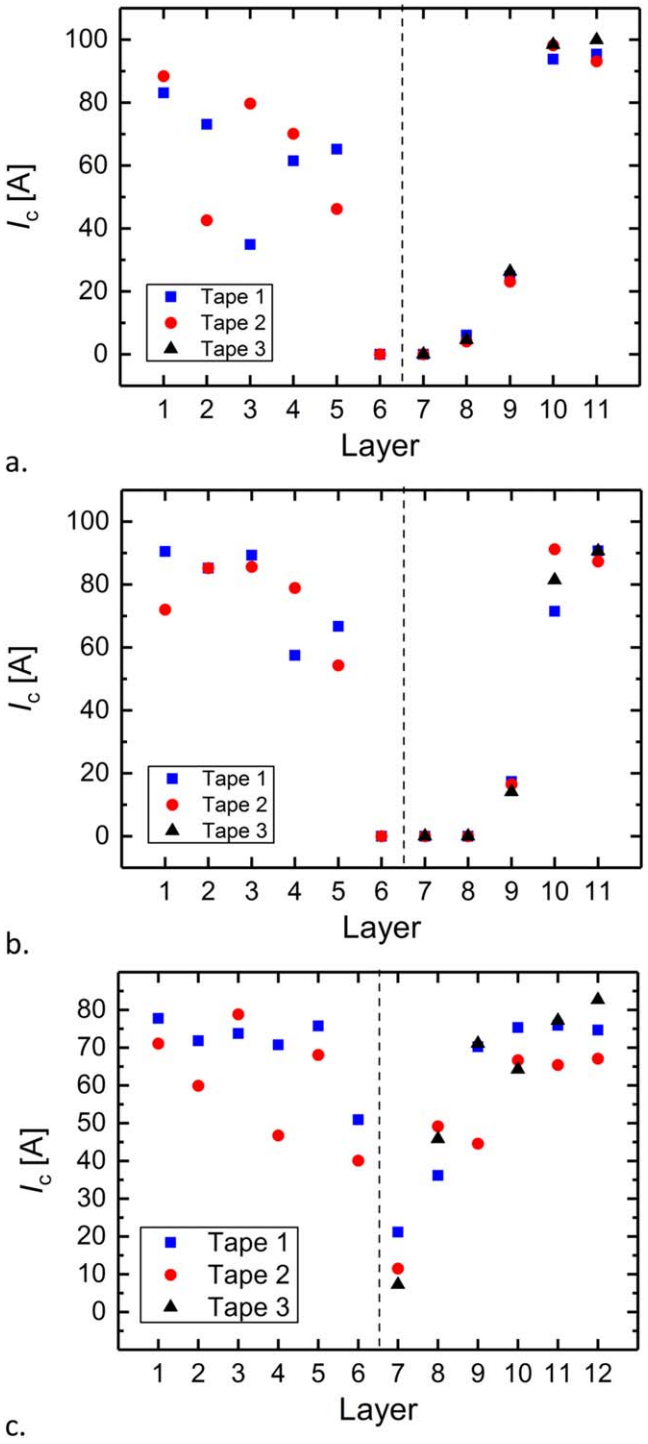

Figure 19. The I_c of tapes extracted from CORC® wire samples after monotonic stress was applied. (a) Sample CORC® 27-1 after monotonic loading to 180 MPa, (b) sample CORC® 27-2 after monotonic loading to 195 MPa, and (c) sample CORC® 30-2 after monotonic loading 200 MPa. The dashed lines indicate the transition from two to three tapes per layer. The tape numbers correspond to the tapes in each layer.

irreversible stress limit. Only once the peak stress exceeded the irreversible stress limit did the critical current degrade with stress cycling.

The combination of relatively high irreversible stress and strain limits already make CORC® wires a highly attractive conductor for magnet applications. A further increase in irreversible stress limit of CORC® wires under axial tension could be realized by replacing the annealed copper former with a cold worked or alloyed copper former, increasing the yield stress of the former to more than 400 MPa at 76 K. Limiting the range of winding angles at which the tapes are wound into the CORC® wire will ensure all tapes are stressed evenly once the former yields, likely causing a further improvement of the irreversible stress limit, but potentially also an even higher irreversible strain limit.

Table 5. Extracted tape and CORC® wire I_c retention.

	σ/σ_{irr} [−]	Tape I_c retention [%]	CORC® wire I_c retention [%]
CORC® 27-1	1.33	51	47
CORC® 27-2	1.41	52	35
CORC® 30-2	1.14	80	67

Acknowledgments

This work has been supported in part by the US Department of Energy under contracts DE-SC0013723, DE-SC0014009 and DE-SC0018125.

ORCID iDs

D C van der Laan https://orcid.org/0000-0001-5889-3751
J D Weiss https://orcid.org/0000-0003-0026-3049

References

[1] Yanagisawa Y *et al* 2015 Combination of high hoop stress tolerance and a small screening current-induced field for an advanced Bi-2223 conductor coil at 4.2K in an external field *Supercond. Sci. Technol.* **28** 125005
[2] Marshall W S, Bird M D, Godeke A, Larbalestier D C, Markiewicz W D and White J M 2017 Bi-2223 test coils for high-resolution NMR magnets *IEEE Trans. Appl. Supercond.* **27** 4300905
[3] Larbalestier D C *et al* 2014 Isotropic round-wire multifilament cuprate superconductor for generation of magnetic fields above 30T *Nat. Mater.* **13** 375–81
[4] Fajardo L G, Brouwer L, Caspi S, Gourlay S, Prestemon S and Shen T 2018 Designs and prospects of Bi-2212 canted-cosine-theta magnets to increase the magnetic field of accelerator dipoles beyond 15T *IEEE Trans. Appl. Supercond.* **28** 40008305
[5] Hazelton D W, Selvamanickam V, Duval J M, Larbalestier D C, Markiewicz W D, Weijers H W and Holtz R L 2009 Recent developments in 2G HTS coil technology *IEEE Trans. Appl. Supercond.* **19** 2218–22
[6] Yoon S, Kim J, Cheon K, Lee H, Hahn S and moon S-H 2016 26T 35 mm all-$GdBa_2Cu_3O_{7-x}$ multi-width no-insulation superconducting magnet *Supercond. Sci. Technol.* **29** 04LT04

[7] Weijers H W 2018 A marriage of high and low temperature superconductors: the 32T magnet *MST Seminar (NHMFL Tallahassee)*

[8] SuperPower Inc. www.superpower-inc.com

[9] Zhang Y, Hazelton D W, Kelley R, Kasahara M, Nakasaki R, Sakamoto H and Polyanskii A 2016 Stress–strain relationship, critical strain (stress) and irreversible strain (stress) of IBAD-MOCVD-based 2G HTS wires under uniaxial tension *IEEE Trans. Appl. Supercond.* **26** 8400406

[10] Apperley M H, Zeng R, Darmann F and McCaughey G 2000 Properties of Ag±Mg alloy sheathed Bi-2223 tapes *Cryogenics* **40** 319–24

[11] Kajbafvala A, Nachtrab W, Wong T and Schwartz J 2014 $Bi_2Sr_2CaCu_2O_{8+x}$ round wires with Ag/Al oxide dispersion strengthened sheaths: microstructure–properties relationships, enhanced mechanical behavior and reduced Cu depletion *Supercond. Sci. Techol.* **27** 095001

[12] Majkic G, Mensah R J, Selvamanickam V, Xie Y-Y and Salama K 2009 Electromechanical behavior of IBAD/MOCVD YBCO coated conductors subjected to torsion and tension loading *IEEE Trans. Appl. Supercond.* **19** 3003–8

[13] ten Haken B, Beuink A and ten Kate H H J 1997 Small and repetitive axial strain reducing the critical current in BSCCO/Ag superconductors *IEEE Trans. Appl. Supercond.* **7** 2034–7

[14] ten Haken B, Godeke A, Schuver H J and ten Kate H H J 1996 Descriptive model for the critical current as a function of axial strain in Bi-2212/Ag wires *IEEE Trans. Appl. Supercond.* **32** 2720–3

[15] Goldacker W, Nast R, Kotzyba G, Schlachter S I, Frank A, Ringsdorf B, Schmidt C and Komarek P 2006 High current DyBCO-ROEBEL assembled coated conductor (RACC) *J. Phys.: Conf. Ser.* **43** 901

[16] Goldacker W, Grilli F, Pardo E, Kario A, Schlachter S I and Vojenčiak M 2014 Roebel cables from REBCO coated conductors: a one-century-old concept for the superconductivity of the future *Supercond. Sci. Technol.* **27** 093001

[17] Takayasu M, Chiesa L, Bromberg L and Minervini J V 2011 Cabling method for high current conductors made of HTS tapes *IEEE Trans. Appl. Supercond.* **21** 2340–4

[18] Takayasu M, Chiesa L, Bromberg L and Minervini J V 2012 HTS twisted stacked-tape cable conductor *Supercond. Sci. Technol.* **25** 014011–21

[19] van der Laan D C 2009 $YBa_2Cu_3O_{7-\delta}$ coated conductor cabling for low ac-loss and high-field magnet applications *Supercond. Sci. Technol.* **22** 065013

[20] van der Laan D C, Lu X F and Goodrich L F 2011 Compact $GdBa_2Cu_3O_{7-\delta}$ coated superconductor cables for electric power transmission and magnet applications *Supercond. Sci. Technol.* **24** 042001

[21] Weiss J D, Mulder T, ten Kate H J J and van der Laan D C 2017 Introduction of CORC® wires: highly flexible, round high-temperature superconducting wires for magnet and power transmission applications *Supercond. Sci. Technol.* **30** 014002

[22] van der Laan D C, Noyes P, Miller G, Weijers H and Willering G 2013 Characterization of a high-temperature superconducting conductor on round core cables in magnetic fields up to 20 T *Supercond. Sci. Technol.* **26** 045005

[23] van der Laan D C, Weiss J D, Noyes P, Trociewitz U P, Godeke A, Abraimov D and Larbalestier D C 2016 Record current density of 344 A/mm^2 at 4.2 K and 17 T in CORC® accelerator magnet cables *Supercond. Sci. Technol.* **29** 055009

[24] van der Laan D C, Weiss J D and McRae D 2019 Status of CORC® cables and wires for use in high-field magnets and power systems a decade after their introduction *Supercond. Sci. Technol.* **32** 033001

[25] Wang X, Caspi S, Dietderich D R, Ghiorso W B, Gourlay S A, Higley H C, Lin A, Prestemon S O, van der Laan D and Weiss J D 2018 A viable dipole magnet concept with REBCO CORC® wires and further development needs for high-field magnet applications *Supercond. Sci. Technol.* **31** 045007

[26] Wang X, Dietderich D R, Marco D, Ghiorso W B, Gourlay S A, Higley H C, Lin A, Prestemon S O, van der Laan D and Weiss J D 2018 Demonstration of 1.2 T canted cos θ dipole magnet using high-temperature superconducting CORC® wires *Supercond. Sci. Technol.* submitted

[27] Nyilas A 2006 Transducers for sub-micron displacement measurements at cryogenic temperatures *AIP Conf. Proc.* **824** 27–34

[28] Mbaruku A L and Schwartz J 2008 Fatigue behavior of Y–Ba–Cu O/hastelloy-C coated conductor at 77 K *IEEE Trans. Appl. Supercond.* **18** 1743–52

[29] Rogers S and Schwartz J 2017 Tensile fatigue behavior and crack growth in $GdBa_2Cu_3O_{7-x}$/stainless-steel coated conductor grown via reactive co-evaporation *Supercond. Sci. Technol.* **30** 045013

[30] Chen W, Zhang H, Chen Y, Liu L, Shi J, Yang X and Zhao Y 2018 Fatigue behavior of critical current degradation for YBCO tapes at 77 K *IEEE Trans. Appl. Supercond.* **28** 8400905

[31] van der Laan D C, McRae D M and Weiss J D 2019 Effect of transverse compressive monotonic and cyclic loading on the performance of superconducting CORC® cables and wires *Supercond. Sci. Technol.* **32** 015002

[32] Cheggour N, Ekin J W, Clickner C C, Verebelyi D T, Thieme C L H, Feenstra R and Goyal A 2003 Reversible axial-strain effect and extended strain limits in Y–Ba–Cu–O coatings on deformation-textured substrates *Appl. Phys. Lett.* **83** 4223–5

[33] van der Laan D C and Ekin J W 2007 Large intrinsic effect of axial strain on the critical current of high temperature superconductors for electric power applications *Appl. Phys. Lett.* **90** 052506

[34] Sugano M, Nakamura T, Manabe T, Shikimachi K, Hirano N and Nagaya S 2008 The intrinsic strain effect on critical current under a magnetic field parallel to the *c* axis for a MOCVD-YBCO-coated conductor *Supercond. Sci. Technol.* **21** 115019

[35] van der Laan D C, Abraimov D, Polyanskii A A, Larbalestier D C, Douglas J F, Semerad R and Bauer M 2011 Anisotropic in-plane reversible strain effect in $Y_{0.5}Gd_{0.5}Ba_2Cu_3O_{7-\delta}$ coated conductors *Supercond. Sci. Technol.* **24** 115010

[36] van der Laan D C, Douglas J F, Goodrich L F, Semerad R and Bauer M 2012 Correlation between in-plane grain orientation and the reversible strain effect on flux pinning in RE-$Ba_2Cu_3O_{7-\delta}$ coated conductors *IEEE Trans. Appl. Supercond.* **22** 8400707

[37] Bumby C W, Badcock R A and Long N J 2013 Critical current behavior of HTS Roebel cable under tensile stress *IEEE Trans. Appl. Supercond.* **23** 4801805

[38] Li Z Y, Li Y Q, Wang M Y, Xi D M, Zhang J W, Ma Y H, Hong Z, Jin Z and Ryu K 2018 Evaluation of electrical and mechanical characteristics for a twisted soldered-stacked-square (3S) HTS wire with 1 mm width *IEEE Trans. Appl. Supercond.* **28** 4800405

[39] Simon N J, Drexler E S and Reed R P 1992 *Properties of Copper and Copper Alloys at Cryogenic Temperatures* NIST Monograph 177 National Institute of Standards and Technology